2026 IEEE/SICE International Symposium on System Integration (SII)
January 11-14, 2026. Cancún, México

Experimental Evaluation of a 3D-Printed Trochoidal Gear Reducer Using Potassium Titanate Fiber-Reinforced Filament*

Chihiro Matayoshi[1], Akifumi Okubo[1], Pauline Barberan[2], Takahiro Aruga[1], and Gen Endo[1]

Abstract— **3D printing technology offers a promising approach for fabricating lightweight and low cost versions of traditionally heavy and expensive components, such as gear reducers. While previous work exists on plastic based reducers, challenges related to low stiffness remain. In this paper, we designed and prototyped a trochoidal gear reducer primarily constructed from a high strength potassium titanate fiber-reinforced material. We conducted a comparative evaluation of two material variants, the nylon based NTL34M and the more stiff PPS based RT4. The experimental results showed no significant difference between the two materials such as no-load running current, joint stiffness, and static torque efficiency. However, in dynamic torque efficiency measurement, the RT4 reducer outperformed the NTL34M version.**

I. INTRODUCTION

In recent years, 3D printing technology has undergone remarkable development, and robot development using thermoplastic materials that leverage this technology is being actively pursued [1]–[4]. Using 3D-printed materials to manufacture robot mechanical parts and structural materials is expected to be an effective means of achieving lighter weight and lower costs compared to conventional metal parts, as well as improving the degree of freedom in component design.

Gear reducers used in robot joints are generally heavy and expensive, contributing to the overall weight and cost of the robot. If these could be manufactured with a 3D printer, a significant effect on weight and cost reduction could be expected. In addition, a higher degree of design freedom leads to the miniaturization of gear reducers and reduction in power consumption through the optimization of the reduction ratio according to requirements. However, as drawbacks, low rigidity and durability are considered.

The development of plastic based gear reducers using 3D printers has been carried out so far, however the strength, particularly gear tooth breakage, has been an issue [5]. To improve gear strength, devising a better shape is one effective method. Trochoidal gears distribute the load over many teeth and have high impact resistance [6], making them suitable for plastic gears in terms of strength. Satake et al. prototyped a reducer with trochoidal gears using 3D-printed parts and conducted a comparative study with metal parts and machined plastic parts through performance evaluation experiments, but the low stiffness of the 3D-printed parts became a clear issue [7].

Therefore, in this paper, we prototype and evaluate the performance of a trochoidal gear reducer mainly made of potassium titanate fiber-reinforced filament (POTICON filament, Otsuka Chemical, hereinafter referred to as POTICON filament), which has high mechanical properties. To the best of our knowledge, POTICON filament has the highest strength and rigidity among short fiber-reinforced plastic materials and is suitable for application to mechanical parts. In this research, we will conduct a comparative study using two types: NTL34M with a nylon base material and RT4 with a Polyphenylene Sulfide, PPS base material. Nylon changes in dimension, strength, and rigidity due to moisture absorption, while PPS does not absorb moisture and has high strength and rigidity, however it also has low impact resistance and is prone to cracking. PPS also has a high glass transition temperature, which traditionally made 3D molding difficult. However, in recent years, 3D printers compatible with PPS based filaments (G-ZERO, GUTENBERG [8], X1E, BambuLab [9]) have become commercially available, making molding possible.

II. DEVELOPMENT OF A TROCHOIDAL GEAR REDUCER

Two types of materials, NTL34M and RT4, were used for the gear reducer. The nominal mechanical properties of NTL34M and RT4 are shown in TABLE I in comparison with Onyx (short carbon fiber-reinforced nylon, Markforged), ABS and PLA [10]–[13]. NTL34M and RT4 are thermoplastic composite materials with nylon and PPS as base plastics, respectively, reinforced with fine potassium titanate fibers. In addition to high strength, they possess micro-reinforcement properties due to microscopically uniform filler dispersion, excellent slidability, and surface smoothness. RT4 is less hygroscopic and features higher rigidity and heat resistance compared to NTL34M.

The operating principle of the trochoidal gear reducer is described below. The rotation of the input shaft is transmitted to the two planetary gears via the eccentric shaft, causing the planetary gears to revolve along the outer ring gear. Here, because a difference is set between the number of teeth on the planetary gears and the number of teeth on the ring gear, the planetary gears perform a rotational motion in the opposite direction of the input, simultaneously with their revolution. This rotational motion is transmitted to the output shaft via pins connected to the planetary gears, resulting in

*This paper is based on results obtained from a project, JPNP14004, commissioned by the New Energy and Industrial Technology Development Organization (NEDO).

[1]Chihiro Matayoshi, Akifumi Okubo, Takahiro Aruga, and Gen Endo are with the Department of Mechanical Engineering, Institute of Science Tokyo, 2-12-1 Ookayama, Meguroku, Tokyo 152-8550, Japan matayoshi.c.ab@m.titech.ac.jp

[2]Pauline Barberan is with the Department of Mechanical Engineering, École d'Ingénieurs SIGMA Clermont, Avenue Blaise Pascal, CS 20265, 63178 Aubière CEDEX, France

the deceleration of the input shaft's rotation. A diagram of the operating principle is shown in Fig. 1.

An overview of the prototyped trochoidal gear reducer is shown in Fig. 2, and its configuration is shown in TABLE II. All parts of the gear reducer, except for bearings, pins, set collars, and insert nuts were fabricated using POTICON filament. For 3D printing, G-ZERO (GUTENBERG) was used for NTL34M, and G-ZERO L1 (GUTENBERG) was used for RT4. The printing conditions are shown in TABLE III. However, to reduce weight, only the ring gear and case had a fill density of 37 % and a triangular fill shape, with some exceptions. Generally, a smaller layer height results in higher strength [14] and allows for cleaner printing of the tooth profile, but since a value that is too small makes fabrication difficult, 0.1 mm was selected. The number of solid layers differed, as these were adopted from the standard profiles provided by the manufacturer for each printer [15]. The G-ZERO profile uses 10 solid layers, while the G-ZERO L1 profile defaults to 8 solid layers. This 8-layer setting is optimized for the L1's larger build stage to prevent warping on the large-scale parts it is typically used for. The planetary gear was fabricated using the method [16], where the 3D printing was paused to press-fit the bearing and then resumed to embed it.

III. EVALUATION OF CHARACTERISTICS

To evaluate the performance of the prototyped trochoidal gear reducer, the no-load running current consumption, joint stiffness, static torque efficiency, and dynamic torque efficiency were investigated. An EPOS2 50/5 (maxon) was used as the motor driver for the experiment. The voltage applied to the motor was 24 V. Grease (MulTemp AC-N, Kyodo Yushi) was applied inside the gear reducer.

A. No-load running current measurement

With the gear reducer attached, the motor was rotated without any external load on the output shaft, and the motor's current consumption was measured. First, the input rotational speed was varied in steps of 1000 rpm within a range of $\pm$ 3000 rpm, which is approximately within half of the motor's own no-load rotational speed, and rotated for 10 seconds at each speed. Next, after continuous operation at a constant speed of 1000 rpm, at the 2-hour and 4-hour

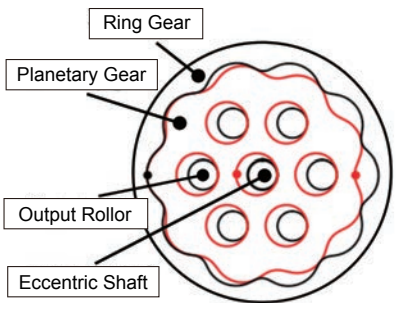

Fig. 1. Schematic diagram of a trochoidal gear reducer

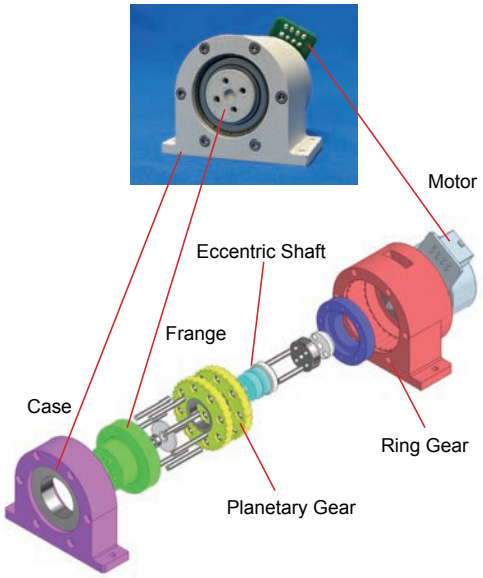

Fig. 2. Overall image of a trochoidal gear reducer

marks, the input rotational speed was similarly varied in steps of 1000 rpm within the $\pm$ 3000 rpm range, and the motor's current consumption was measured at each speed. The measurement was performed twice, and the average value was calculated.

The results for the NTL34M reducer are shown in Fig. 3, and for the RT4 reducer in Fig. 4. From the results, it was found that the current consumption decreased after 2 hours of operation for both reducers. This is thought to be because irregularities on the tooth surfaces from printing were worn down. After 2 hours, the current consumption of the NTL34M and RT4 versions was comparable. The current consumption at this time was about 500 mA. Given that the motor's no-load current is 270 mA [17] and the applied

TABLE I
MECHANICAL PROPERTIES OF THE MATERIALS

Material	NTL34M	RT4	Onyx	ABS	PLA
Base material	Nylon	PPS	Nylon	ABS	PLA
Tensile strength [MPa]	114	110	37	38	45
Bending strength [MPa]	199	210	71	61	92
Flexural modulus [GPa]	7.0	9.7	3.0	1.4	2.9
Heat deflection temperature (°C) @0.45 MPa	129.9	266.8	145	87	58

TABLE II
CONFIGULATION OF A TROCHOIDAL GEAR REDUCER

Motor	Brushless DC motor (EC 45 flat 80 W, Maxon Japan)
Gear ratio	30
Metal parts	Bearings, pins, set collars, screws, insert nuts
POTICON filament parts	All other components

TABLE III
PARAMETERS FOR THE 3D PRINTING

Material	NTL34M	RT4
3D printer	G-ZERO	G-ZERO L1
Slicer	PrusaSlicer	PrusaSlicer
Nozzle diameter [mm]	0.4	0.4
Extruder temperature [°C] (first layer / subsequent layers)	270 / 270	340 / 320
Layer height [mm]	0.1	0.1
Number of shells	2	2
Number of solid layers (top / bottom)	10 / 10	8 / 8
Fill density	100%	100%
Fill shape	Concentric	Concentric

voltage is 24 V, the loss due to the reducer is considered to be approximately 5.5 W.

B. Joint stiffness measurement

Next, the joint stiffness was investigated by applying a load while the joint was held horizontally. A schematic of the joint stiffness measurement is shown in Fig. 5. An aluminum pipe was attached to the output shaft of the reducer, and a load torque was applied by hanging a weight at its tip. The vertical displacement of the pipe's tip from a horizontally held position was measured on the upper surface of a 3D-printed fixture attached to the pipe's tip using a laser displacement sensor (LK-H150, Keyence). Prior to measurement, after performing position control to make the aluminum pipe parallel to the mount, the motor's outer rotor was fixed by a clamp. As a load, weights were applied sequentially from 0 N to 4 N in 1 N increments, and the test was conducted in a cycle of similarly unloading them. At each load stage, after placing the weight and letting it rest for 1 minute, the displacement was measured for 10 seconds. The measurement was performed twice, and the average value was calculated.

The results are shown in Fig. 6. By performing linear interpolation from the graph and converting the displacement to the joint angle by approximating it as the length of an arc, the moment stiffness of the NTL34M reducer was 208 Nm/rad, and that of the RT4 reducer was 209 Nm/rad. For reference, a Harmonic Drive (CSF-14-30-2A-R, Harmonic Drive Systems) with a similar outer diameter and a reduction ratio of 30 has a stiffness of 1900 Nm/rad [18]. From the results, it was shown that the joint stiffness of the NTL34M and RT4 reducers is comparable. In addition, no difference was observed in the hysteresis characteristics in the loading and unloading cycles.

C. Static torque measurement

Next, the efficiency of the output torque under stationary conditions was investigated. A schematic of the static torque measurement is shown in Fig. 7. An aluminum pipe was attached to the output shaft of the reducer, and a digital scale (SJ-5000, A&D) was placed to make contact with the aluminum pipe at a horizontal position relative to the

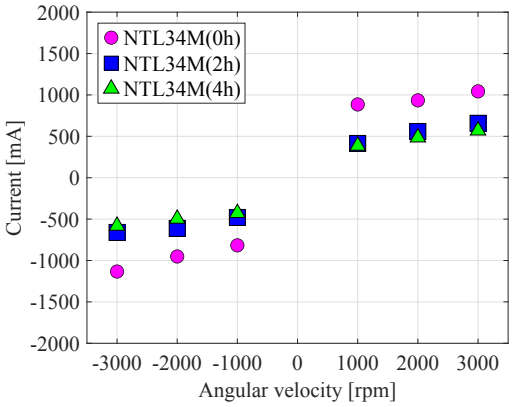

Fig. 3. No-load running current of NTL34M gear reducer

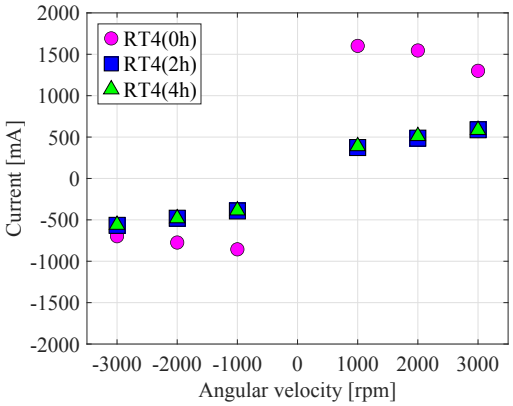

Fig. 4. No-load running current of RT4 gear reducer

ground. The torque measurement method involves applying a constant commanded current to the motor, converting the output value of the scale pressed by the aluminum pipe into a force, and multiplying it by the arm length (300 mm) from the output shaft to the contact point with the scale to obtain the static torque value. The measurement was performed 5 times, and the average value was calculated.

The results are shown in Fig. 8. The horizontal axis represents the command torque value calculated from the motor's current command value, the torque constant (40.4 mNm/A [17]), and the gear ratio. The vertical axis shows the efficiency, which is the measured static torque value divided by the value on the horizontal axis. The results showed that the static torque efficiency was comparable between the NTL34M and RT4 versions. The efficiency was about 70-90 %, and notably, for command torque values of 2 Nm or less, the efficiency was 80 % or higher.

D. Dynamic torque measurement

Finally, the efficiency of the output torque during rotation was investigated. A schematic of the dynamic torque measurement is shown in Fig. 9. A micro powder brake (OPB80N, Ogura Clutch) was attached to the output of the reducer to apply a load torque. The magnitude of the load torque output by the micro powder brake is determined by

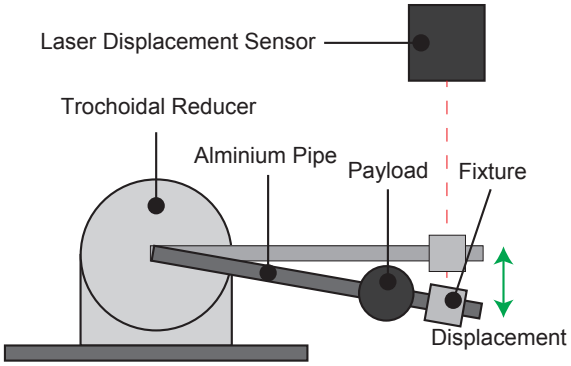

Fig. 5. Experimental apparatus for joint stiffness measurement

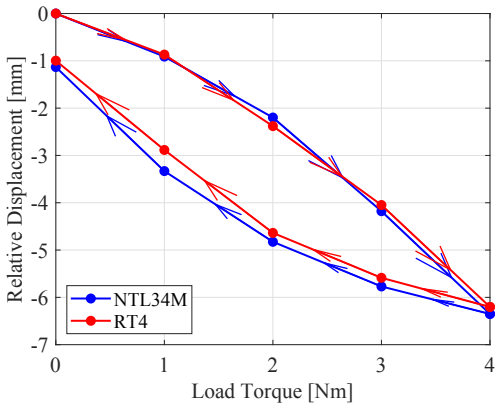

Fig. 6. Experimental results on joint stiffness

the value of the excitation current applied to the brake, and the brake can output a load torque from 0.5 Nm to 8 Nm. The relationship between the excitation current applied to the micro powder brake and its output torque was investigated prior to the experiment. The reducer output shaft was attached to the micro powder brake, and while the micro powder brake output a load torque, the motor was rotated at a constant speed. The output torque of the reducer was calculated by multiplying the current flowing to the motor by the torque constant and the gear ratio, and the efficiency was taken as the load torque relative to the reducer's output torque. The load torque was varied, and

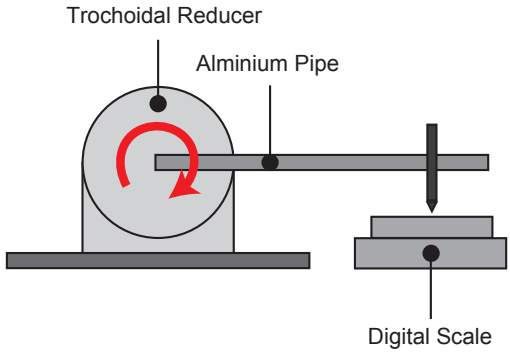

Fig. 7. Experimental apparatus for static torque measurement

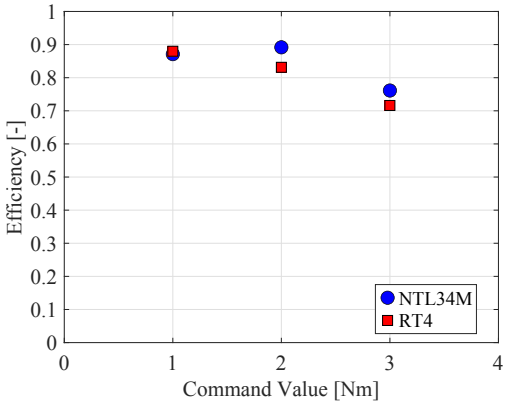

Fig. 8. Static torque efficiency

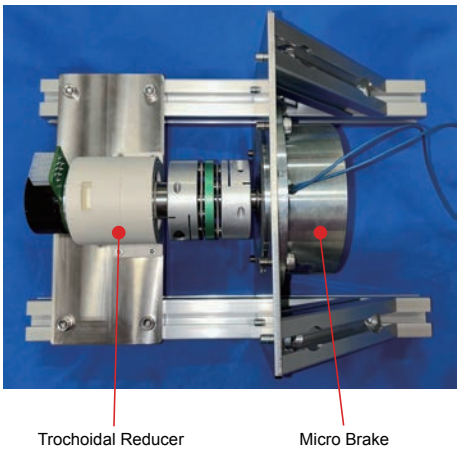

Fig. 9. Experimental apparatus for dynamic torque measurement

the efficiency was measured. The experiment was conducted with motor rotation speed command values of 400, 1000, 2000, and 3000 rpm. The measurement of the motor's current consumption was started after it settled to a speed close to the commanded rotational speed, excluding the motor's start-up phase. The measurement duration was 10 seconds, and the average current flowing was calculated. The measurement was performed twice.

The results are shown in Fig. 10. The horizontal axis shows the magnitude of the load torque from the brake, and the vertical axis shows the efficiency. From the results, the RT4 version showed higher maximum efficiency than the NTL34M version at all rotational speeds. The maximum efficiency at each rotational speed is shown in TABLE IV. The value in parentheses is the torque at which maximum efficiency was shown. From the maximum efficiency results, it was confirmed that in the measurement range where the reducer rotates stably, the maximum efficiency of the NTL34M version was approximately 60 %, and that of the RT4 version was approximately 70 %.

IV. DISCUSSION

Based on the results of the performance evaluation experiments, the NTL34M and RT4 versions are compared. The experimental results are summarized below.

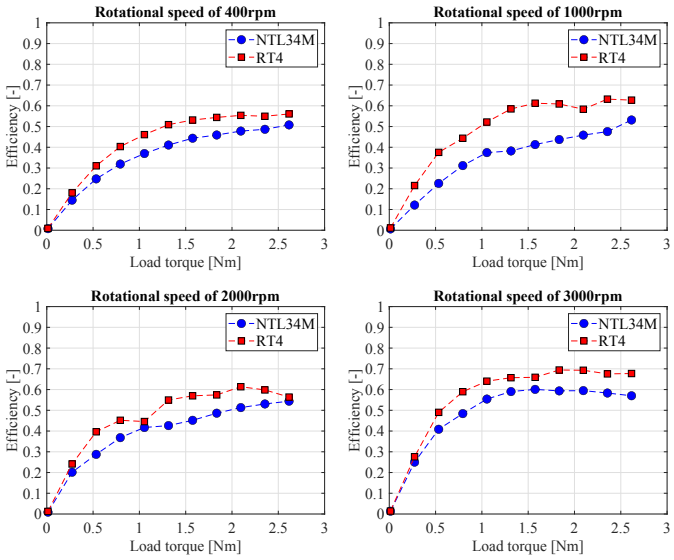

Fig. 10. dynamic torque efficiency

TABLE IV
MAXIMUM DYNAMIC TORQUE EFFICIENCY

Rotational Speed [rpm]	NTL34M	RT4
400	51 % (2.6 Nm)	56 % (2.6 Nm)
1000	53 % (2.6 Nm)	63 % (2.4 Nm)
2000	54 % (2.6 Nm)	61 % (2.1 Nm)
3000	60 % (2.6 Nm)	69 % (2.1 Nm)

- During no-load rotation, the NTL34M and RT4 versions consumed a similar amount of current. The loss due to the reducer is considered to be approximately 5.5 W.
- The joint stiffness of the reducers was comparable for both versions.
- The static torque efficiency of the reducers was comparable for both versions, at about 70-90 %. In particular, for command torque values of 2 Nm or less, the efficiency was 80 % or higher.
- The dynamic torque efficiency of the RT4 version was higher than that of the NTL34M version; the maximum efficiency was approximately 60 % for the NTL34M version and approximately 70 % for the RT4 version.

In the static evaluations, the NTL34M and RT4 reducers showed comparable performance. Although RT4 is superior in terms of material stiffness, it is considered that this difference does not significantly affect the static characteristics of the prototyped reducer. On the other hand, the RT4 version surpassed the NTL34M version in dynamic torque efficiency. This suggests that during operation, the material's stiffness affects efficiency.

V. CONCLUSION

In this paper, we prototyped and evaluated the performance of trochoidal gear reducers mainly made of NTL34M and RT4, respectively. From the results of the performance evaluation, no-load running current, joint stiffness, and static torque efficiency of the NTL34M and RT4 models were comparable. On the other hand, the dynamic torque efficiency of the RT4 model was superior. Future work will involve examining how the characteristics of NTL34M and RT4 change with moisture absorption. Currently, we are proceeding with the evaluation of durability for mounting on a robot [19]. In a durability test in which the NTL34M model was operated with a weight attached so that a maximum load of 4 Nm was applied, operation for about 929 hours was confirmed. We will proceed with the evaluation of the RT4 model in the future. Furthermore, we will investigate the high degree of design freedom by prototyping models with different gear ratios. We will also prototype reducers that are lightweight by adjusting printing parameters, such as layer height, and implementing design modifications for weight reduction. Finally, we will evaluate their potential to substitute for conventional metal gear reducers.

ACKNOWLEDGMENT

This paper is based on results obtained from a project, JPNP14004, commissioned by the New Energy and Industrial Technology Development Organization (NEDO).

We thank Otsuka Chemical Co., Ltd. for providing materials and information and for their advice in writing this paper. We also thank GUTENBERG Co., Ltd. for their cooperation and advice regarding 3D printing.

We thank Prof. Naoyuki Takesue (Tokyo Metropolitan University), Prof. Yusuke Ota (Chiba Institute of Techonology), and Prof. Takeshi Takaki (Hiroshima University) for their valuable comments and discussion.

REFERENCES

[1] J. Kim, T. Kang, D. Song, and S.-J. Yi, "Design and control of a open-source, low cost, 3d printed dynamic quadruped robot," *Applied Sciences*, vol. 11, no. 9, p. 3762, 2021.

[2] S. Mick, M. Lapeyre, P. Rouanet, C. Halgand, J. Benois-Pineau, F. Paclet, D. Cattaert, P.-Y. Oudeyer, and A. de Rugy, "Reachy, a 3d-printed human-like robotic arm as a testbed for human-robot control strategies," *Frontiers in neurorobotics*, vol. 13, p. 65, 2019.

[3] F. Sanfilippo, E. Helgerud, P. A. Stadheim, and S. L. Aronsen, "Serpens: A highly compliant low-cost ros-based snake robot with series elastic actuators, stereoscopic vision and a screw-less assembly mechanism," *Applied Sciences*, vol. 9, no. 3, p. 396, 2019.

[4] A. Bulgarelli, G. Toscana, L. O. Russo, G. A. Farulla, M. Indaco, and B. Bona, "A low-cost open source 3d-printable dexterous anthropomorphic robotic hand with a parallel spherical joint wrist for sign languages reproduction," *International Journal of Advanced Robotic Systems*, vol. 13, no. 3, p. 126, 2016.

[5] T. Yoshida, G. Endo, A. Okubo, and H. Nabae, "Experimental evaluation of a quasi-direct-drive actuator with a 3d-printed planetary gear reducer," in *2023 IEEE/SICE International Symposium on System Integration (SII)*. IEEE, 2023, p. 1.

[6] L. Ivanović, "Reduction of the maximum contact stresses by changing geometric parameters of the trochoidal gearing teeth profile," *Meccanica*, vol. 51, no. 9, p. 2243, 2016.

[7] H. Satake and N. Takesue, "Comparison of characteristics of cycloidal gear reducer using metal, plastic and 3d printed parts," in *2024 IEEE/SICE International Symposium on System Integration (SII)*. IEEE, 2024, p. 1531.

[8] (2025) G-zero. Gutenberg Inc. Accessed: August 8, 2025. [Online]. Available: https://gutenberg.co.jp/en/products/g-zero-1

[9] (2025) X1e. Bambu Lab. Accessed: August 8, 2025. [Online]. Available: https://bambulab.com/en/x1e

[10] (2025) Filament for 3d printer. Otsuka Chemical Co., Ltd. Accessed: August 1, 2025. [Online]. Available: https://www.otsukac.co.jp/en/products/cat-composite-resin/filament.html

[11] (2025) Composites material datasheet. Markforged, Inc. Accessed: August 8, 2025. [Online]. Available: https://s3.amazonaws.com/mf.product.doc.images/Datasheets/Material+Datasheets/CompositesMaterialDatasheet.pdf
[12] (2025) Ultimaker abs tds. Ultimaker B.V. Accessed: August 1, 2025. [Online]. Available: https://support.ultimaker.com/hc/en-us/articles/360012759139-Ultimaker-ABS-TDS
[13] (2025) Ultimaker tough pla tds. Ultimaker B.V. Accessed: August 1, 2025. [Online]. Available: https://support.ultimaker.com/hc/en-us/articles/360012759599-Ultimaker-Tough-PLA-TDS
[14] V. E. Kuznetsov, A. N. Solonin, O. D. Urzhumtsev, R. Schilling, and A. G. Tavitov, "Strength of pla components fabricated with fused deposition technology using a desktop 3d printer as a function of geometrical parameters of the process," *Polymers*, vol. 10, no. 3, p. 313, 2018.
[15] (2025) Installing and initial setup of prusaslicer. GUTENBERG Co., Ltd. Accessed: November 14, 2025. [Online]. Available: https://support.gutenberg.co.jp/hc/ja/articles/45305358220313-PrusaSlicer%E3%81%AE%E3%82%A4%E3%83%B3%E3%82%B9%E3%83%88%E3%83%BC%E3%83%AB%E3%81%A8%E5%88%9D%E6%9C%9F%E8%A8%AD%E5%AE%9A
[16] K. Kanazawa, H. Nabae, K. Suzumori, and G. Endo, "Mechanical parts manufactured by a 3d printer for industrial robot -part3 : Proposal of assembly during modeling and stacking draft-," in *Proceedings of the 2022 JSME Conference on Robotics and Mechatronics*, 2022, p. 2P1-L08, in Japanese.
[17] (2025) EC 45 flat 80 W. maxon group. Accessed: August 1, 2025. [Online]. Available: https://www.maxongroup.com/maxon/view/product/591480
[18] (2025) Technical documents / catalogs. Harmonic Drive Systems Co., Ltd. Accessed: November 12, 2025. [Online]. Available: https://www.hds.co.jp/products/pdf.html?catid=63&type=1
[19] A. Okubo, H. Nabae, and G. Endo, "Mechanical parts manufactured by a 3d printer for industrial robot -part7 : Improving the durability of resin trochoidal reducer-," in *Proceedings of the 24th SICE System Integration Division Annual Conference*, 2023, p. 931, in Japanese.